



This discussion paper is/has been under review for the journal The Cryosphere (TC).  
Please refer to the corresponding final paper in TC if available.

# A recent bifurcation in Arctic sea-ice cover

V. N. Livina<sup>1</sup> and T. M. Lenton<sup>2</sup>

<sup>1</sup>School of Environmental Sciences, University of East Anglia, Norwich NR4 7TJ, UK

<sup>2</sup>College of Life and Environmental Sciences, University of Exeter, Exeter EX4 4PS, UK

Received: 26 June 2012 – Accepted: 2 July 2012 – Published: 18 July 2012

Correspondence to: V. N. Livina (v.livina@uea.ac.uk)

Published by Copernicus Publications on behalf of the European Geosciences Union.

## A recent bifurcation in Arctic sea-ice cover

V. N. Livina and  
T. M. Lenton

Title Page

Abstract

Introduction

Conclusions

References

Tables

Figures

◀

▶

◀

▶

Back

Close

Full Screen / Esc

Printer-friendly Version

Interactive Discussion



## Abstract

There is ongoing debate over whether Arctic sea-ice has already passed a “tipping point”, or whether it will do so in future, with several recent studies arguing that the loss of summer sea ice does not involve a bifurcation because it is highly reversible in models. Recently developed methods can detect and sometimes forewarn of bifurcations in time-series data, hence we applied them to satellite data for Arctic sea-ice cover. Here we show that a new low ice cover state has appeared from 2007 onwards, which is distinct from the normal state of seasonal sea ice variation, suggesting a bifurcation has occurred from one attractor to two. There was no robust early warning signal of critical slowing down prior to this bifurcation, consistent with it representing the appearance of a new ice cover state rather than the loss of stability of the existing state. The new low ice cover state has been sampled predominantly in summer-autumn and seasonal forcing combined with internal climate variability are likely responsible for triggering recent transitions between the two ice cover states. However, all early warning indicators show destabilization of the summer-autumn sea-ice since 2007. This suggests the new low ice cover state may be a transient feature and further abrupt changes in summer-autumn Arctic sea-ice cover could lie ahead; either reversion to the normal state or a yet larger ice loss.

## 1 Introduction

Arctic sea-ice has experienced striking reductions in areal coverage (Stroeve et al., 2007; Nghiem et al., 2007), especially in recent summers, with 2007–2011 having the five lowest ice cover minima in the satellite record (Fig. 1). Observations have fallen below IPCC model projections (Stroeve et al., 2007), despite the models having been in agreement with the observations in the 1970s. Summer ice cover is forecast to disappear later this century (Boe et al., 2009), but the nature of the underlying transition is

## A recent bifurcation in Arctic sea-ice cover

V. N. Livina and  
T. M. Lenton

[Title Page](#)

[Abstract](#)

[Introduction](#)

[Conclusions](#)

[References](#)

[Tables](#)

[Figures](#)

◀

▶

[Back](#)

[Close](#)

[Full Screen / Esc](#)

[Printer-friendly Version](#)

[Interactive Discussion](#)



debated (Lenton et al., 2008; Lindsay and Zhang, 2005; Amstrup et al., 2010; Winton, 2006; Eisenman and Wettlaufer, 2009; Tietsche et al., 2011).

Arctic sea-ice has been identified as a potential tipping element in the Earth's climate system (Lenton et al., 2008), and at least one study suggests it has already passed a "tipping point" (Lindsay and Zhang, 2005). In the future, some models forecast abrupt ice loss events (Amstrup et al., 2010), on the way to a seasonally ice-free Arctic. These may qualify as passing tipping points following the definition in Lenton et al. (2008), which includes both reversible and irreversible transitions. However, most recent papers address whether summer sea-ice loss will involve an irreversible (e.g. saddle-node/fold) bifurcation, and they find instead that in models the loss of summer sea-ice cover is highly reversible (Amstrup et al., 2010; Winton, 2006; Eisenman and Wettlaufer, 2009; Tietsche et al., 2011). Abrupt ice loss events are then attributed to the loss of year-round sea-ice in the Arctic making the remaining ice more vulnerable to summer melt, and prone to larger fluctuations in area coverage (Notz et al., 2009). One exception is a recent model (Abbot et al., 2011) showing that positive feedbacks involving clouds can create multiple stable states for seasonal ice cover and bifurcations between them.

Here we attempt to resolve whether the Arctic sea-ice is approaching, or has passed, a bifurcation point by applying methods of time-series analysis that can detect (Livina et al., 2010, 2011b) and in some cases forewarn (Scheffer et al., 2009; Held and Kleinen, 2004; Livina and Lenton, 2007; Lenton, 2011) of bifurcations. We analyse the satellite-derived daily record of sea-ice area from 1979 to present (Fig. 1a), and repeat the analysis on sea-ice extent data (Eisenman, 2010) (Fig. A1) in the Appendix. For our analysis, the mean seasonal cycle (Fig. 1b) is removed from the data, because there is a very strong seasonally-forced variation in sea-ice area, but we are interested in the behavior of fluctuations from this typical state of seasonal variation. The last five years have been characterized by an increase in the amplitude of seasonal sea-ice variation (Fig. 1a), as the annual ice cover minimum dropped the order of  $\sim 10^6 \text{ km}^2$  more than the annual maximum in 2007 and the difference has been maintained since

## A recent bifurcation in Arctic sea-ice cover

V. N. Livina and  
T. M. Lenton

[Title Page](#)

[Abstract](#) [Introduction](#)

[Conclusions](#) [References](#)

[Tables](#) [Figures](#)

[◀](#) [▶](#)

[◀](#) [▶](#)

[Back](#) [Close](#)

[Full Screen / Esc](#)

[Printer-friendly Version](#)

[Interactive Discussion](#)



then (Fig. 1c). This already hints that a new attractor for summer-autumn sea-ice cover may have been sampled in the last 5 yr.

## 2 Methodology

### 2.1 Data and pre-processing

- 5 Sea-ice area takes into account the fraction of a grid cell (above 15 %) that is covered by sea ice, and can be biased low, especially in summer when melt ponds are present. Sea-ice extent assumes that any grid point with more than 15 % sea ice concentration is totally covered, hence it is biased high.

Sea ice area data was obtained from “The Cryosphere Today” project of the University of Illinois. This dataset (<http://arctic.atmos.uiuc.edu/cryosphere/timeseries.anom.1979-2008>) uses SSM/I and SMMR series satellite products and spans 1979 to present at daily resolution. The mean seasonal cycle over 1979–2008 is removed, which is the standard convention. The most recent data in this series is derived from the Near-Real-Time DMSP SSM/I-SSMIS Daily Polar Gridded Sea Ice Concentrations of the National 15 Snow & Ice Data Centre (NSIDC) (see Maslanik and Stroeve, 1999).

The sea-ice extent time series was derived by Eisenman (Eisenman, 2010) (data available from <ftp://ftp.agu.org/apend/gl/2010gl043741>) on the basis of sea ice concentration using the NASA Team algorithm from Nimbus-7 SMMR (1978–1987), DMSP SSM/I (1987–2009), and DMSP SSMIS (2008–present) satellite passive microwave 20 radiances on a 25×25 km polar stereographic grid (Cavalieri et al., 1996; Meier et al., 2006; Maslanik and Stroeve, 1999). During periods of instrumental transitions, the overlapping datasets were averaged. Extent was calculated by summing the areas of all grid boxes with at least 15 % ice concentration. Details of the spatial data interpolation are given by Eisenman (2010). The time series spans 1979–2009, and where 25 it has 2-day resolution (when SMMR operated every other day in three months during the record, in 10/1978, 12/1987 and 1/1988), we interpolate to daily resolution to obtain

TCD

6, 2621–2651, 2012

## A recent bifurcation in Arctic sea-ice cover

V. N. Livina and  
T. M. Lenton

Title Page

Abstract

Introduction

Conclusions

References

Tables

Figures

◀

▶

◀

▶

Back

Close

Full Screen / Esc

Printer-friendly Version

Interactive Discussion



a homogeneous time-series, before removing the mean seasonal cycle. We also analyzed a derived index of “equivalent sea-ice extent” (Eisenman, 2010) (available from <ftp://ftp.agu.org/pend/gl/2010gl043741>), which is based on the latitude of the sea-ice edge where it is free to migrate, converted to an area, assuming there were no continents present.

## 2.2 Potential analysis

To detect any bifurcations in the sea-ice data, we use a recently-developed (Livina et al., 2010, 2011b) and rigorously blind-tested (Livina et al., 2011a) method of “potential analysis”. This assumes that a system is experiencing sufficient short-term stochastic variability (noise) that it is sampling all of its available states or attractors (given a sufficiently long time window). Then we take advantage of the fact that the stationary probability distribution of the resulting data is directly related to the shape of the underlying potential, which describes the number of underlying system states and their stability (Livina et al., 2011b). Thus, with a sufficiently long time window of data one can deduce the number of system states and their relative stability or instability.

The time series are modelled by the stochastic differential equation:

$$\dot{z}(t) = -U'(z) + \sigma\eta, \quad (1)$$

where  $U$  is a polynomial potential of even order,  $\eta$  is a Gaussian white noise process of unit variance. Equation (1) has a corresponding Fokker-Planck equation describing the probability density function, and crucially this has a stationary solution that depends only on the underlying potential function and the noise level,  $\sigma$ ;

$$p(z) \sim \exp \frac{-2U(z)}{\sigma^2}. \quad (2)$$

TCD

6, 2621–2651, 2012

## A recent bifurcation in Arctic sea-ice cover

V. N. Livina and  
T. M. Lenton

Title Page

Abstract

Introduction

Conclusions

References

Tables

Figures

◀

▶

◀

▶

Back

Close

Full Screen / Esc

Printer-friendly Version

Interactive Discussion



This allows the underlying potential to be reconstructed from a kernel probability distribution of time-series data (and an estimate of the noise level) as:

$$U(z) = -\frac{\sigma^2}{2} \log p_d(z), \quad (3)$$

where  $p_d$  is the empirical probability density of the data.

We detect the order of the polynomial and hence the number of system states following the method in Livina et al. (2010, 2011b), plotting the results as a function of window length at the end of each sliding window in a colour contour plot (e.g., Fig. 3b). The rate of correct detection depends on sliding window size (Livina et al., 2011b): when the window contains more than 400 data points (which in the case of daily sea-ice data corresponds to about 1.1 yr), the success rate is 80 %, even when noise level is up to five times bigger than the depth of the potential well; for larger windows it approaches 98 %. A test of the method on artificial data, generated from a model system in which the underlying potential bifurcates from one state to two, illustrates correct detection of the number of system states (Fig. 2).

We derive the coefficients describing the shape of the potential using an unscented Kalman filter (Livina et al., 2010, 2011b), while we estimate the noise level using wavelet de-noising with Daubechies wavelets of 4th order (Livina et al., 2011b).

The method assumes each subset of data is quasi-stationary and the noise is Gaussian white. For the 4-yr intervals used to reconstruct the potentials in Fig. 3c, the assumption of stationarity is reasonable. The noise in geophysical systems may be red rather than white, but the assumption of white noise can still be valid provided that the noise is stationary (DFA fluctuation exponent less than 1). By applying the potential model in such cases, we may attribute part of noise variability to the potential dynamics when analysing the two components of the potential model. This model is an approximation; still it allows us to derive accurately the structure of the potential for systems with stationary red noise. When there are no non-stationarities such noise cannot artificially create an additional system state.

## A recent bifurcation in Arctic sea-ice cover

V. N. Livina and  
T. M. Lenton

[Title Page](#)

[Abstract](#)

[Introduction](#)

[Conclusions](#)

[References](#)

[Tables](#)

[Figures](#)

◀

▶

◀

▶

[Back](#)

[Close](#)

[Full Screen / Esc](#)

[Printer-friendly Version](#)

[Interactive Discussion](#)



## 2.3 Critical slowing down

For a low-order dynamical system approaching a bifurcation where its current state becomes unstable, and it transitions to some other state, one can expect to see it become more sluggish in its response to small perturbations (Scheffer et al., 2009). This can hold even for complex systems such as the sea-ice, because near to a bifurcation point their behavior reduces down to that of a low-order system (following the Center Manifold Theorem). This signal of “critical slowing down” (Scheffer et al., 2009) is detectable as increasing autocorrelations in time series data, occurring over timescales capturing the decay of the major mode in the system (Held and Kleinen, 2004), which is controlled by the leading eigenvalue. We looked for this early warning indicator in the form of rising lag-1 autocorrelation (Held and Kleinen, 2004) (ACF-indicator), and through detrended fluctuation analysis (DFA-indicator) as a rising scaling exponent (Livina and Lenton, 2007). Parabolic trends were removed prior to estimating these two indicators (previously termed “propagators”; Held and Kleinen, 2004; Livina and Lenton, 2007) of critical slowing down. This is because any trend affects autocorrelations and hence may cause false positive signals in the indicators. To test robustness we also performed an alternative pre-processing of data; first removing the quadratic downward trend and then deseasonalising the data, and obtained equivalent results.

### 2.3.1 ACF-indicator

Lag-1 autocorrelation was estimated (Held and Kleinen, 2004; Livina and Lenton, 2007) by fitting an autoregressive model of order 1 (linear AR(1)-process) of the form:

$$z_{t+1} = c \cdot z_t + \sigma \eta_t, \quad (4)$$

where  $\eta_t$  is a Gaussian white noise process of unit variance, and the “ACF-indicator” (AR1 coefficient):

$$c = e^{-\kappa \Delta t}, \quad (5)$$

## A recent bifurcation in Arctic sea-ice cover

V. N. Livina and  
T. M. Lenton

[Title Page](#)

[Abstract](#)

[Introduction](#)

[Conclusions](#)

[References](#)

[Tables](#)

[Figures](#)

◀

▶

◀  
Back

▶  
Close

[Full Screen / Esc](#)

[Printer-friendly Version](#)

[Interactive Discussion](#)



where  $\kappa$  is the decay rate of perturbations, and  $\kappa \rightarrow 0$  (i.e.  $c \rightarrow 1$ ) as bifurcation is approached (Held and Kleinen, 2004).

### 2.3.2 DFA-indicator

Detrended fluctuation analysis (DFA) extracts the fluctuation function of window size  $s$ , which increases as a power law if the data series is long-term power-law correlated:

$$F(s) \propto s^\alpha \quad (6)$$

where  $\alpha$  is the DFA scaling exponent. In the short-term regime, as  $c \rightarrow 1$  of the AR(1)-model, the slowing exponential decay is well approximated by a power law in which  $\alpha \rightarrow 1.5$ , in the time interval 10–100 units. Exponent  $\alpha$  is rescaled, following Livina and Lenton (2007), to give a “DFA-indicator” that reaches 1 at critical behavior.

### 2.3.3 Variance

We also monitored variance (calculated as standard deviation), because if a state is becoming less stable this can be characterized by its potential well getting shallower, causing increased variability over time (although this is not independent of lag-1 auto-correlation, Ditlevsen and Johnsen, 2010).

### 2.3.4 Indicator trends

Upward trends in the indicators (rather than their absolute value) provide the primary early warning signal. The Kendall  $\tau$  rank correlation coefficient (Kendall, 1948) measures the strength of the tendency of an indicator to increase (positive values) or decrease (negative values) with time, against the null hypothesis of a random sequence of measurements against time (value approximately zero). As a sensitivity analysis, the sliding window along the time series was varied from 1/4 to 3/4 of the series length.

[Title Page](#)[Abstract](#)[Introduction](#)[Conclusions](#)[References](#)[Tables](#)[Figures](#)[◀](#)[▶](#)[◀](#)[▶](#)[Back](#)[Close](#)[Full Screen / Esc](#)[Printer-friendly Version](#)[Interactive Discussion](#)

### 3 Results and discussion

#### 3.1 Bifurcation detection

After removing the mean seasonal cycle, the remaining fluctuations in sea-ice area include some of order  $10^6 \text{ km}^2$  (Fig. 3a). The largest anomalies are in 1996 (maximum of the series) and 2007–2011 (minima). They typically occur in the summer-autumn, when the sea-ice area is at its lowest in the seasonal cycle. Given the size of sea-ice fluctuations during 2007–2011 (Fig. 3a) and the pronounced drop in sea-ice minima relative to sea-ice maxima since 2007 (Fig. 1c), we considered whether a new, lower sea ice cover state has started to appear.

On analyzing the sea-ice area data using our method of potential analysis, over long time windows (here  $>1 \text{ yr}$ ), we typically find a single sea-ice state, representing the normal seasonal cycle of variability (Fig. 3b). Sometimes a second state is detected associated with e.g., the sea-ice maximum in 1996, but these changes are not found simultaneously and persistently across a wide range of window lengths. However, from 2007 onwards, a persistent switch to two states in sea-ice cover fluctuations is detected, across a wide range of window lengths up to  $>10 \text{ yr}$  (Fig. 3b). The same switch is also detected in analysis of sea-ice extent data (Fig. A2).

The stability of the sea-ice state(s) can be reconstructed, in the form of potential curves for fixed intervals of the data (Fig. 3c), with associated error estimates (on the coefficients of the polynomial function describing the potential, Livina et al., 2011b). The sea-ice is typically characterized by a single stable state. The interval 1996–1999 (including the 1996 maximum anomaly) shows signs of a second high ice state that is degenerate (i.e. not fully stable). In 2000–2003 there is a return to a single state. In 2004–2007, which includes the record September 2007 sea-ice retreat, a low ice-cover state starts to appear. Then in 2008–2011 the potential separates into two stable states, although the error range allows for one or the other of these to be degenerate. The potential curves are derived from histograms of the original data (Livina et al., 2011b) (Fig. 3d), which confirm a second mode appearing among a long tail of negative

TCD

6, 2621–2651, 2012

#### A recent bifurcation in Arctic sea-ice cover

V. N. Livina and  
T. M. Lenton

[Title Page](#)

[Abstract](#)

[Introduction](#)

[Conclusions](#)

[References](#)

[Tables](#)

[Figures](#)

◀

▶

◀

▶

[Back](#)

[Close](#)

[Full Screen / Esc](#)

[Printer-friendly Version](#)

[Interactive Discussion](#)



fluctuations during 2004–2007, followed by a separation of modes during 2008–2011. Thus, we argue that Arctic sea-ice recently passed a bifurcation point, which created a new lower ice cover state. Since then it has fluctuated between its normal state of seasonal variability and the new, lower ice cover state.

### 5 3.2 Early warnings?

Having detected a bifurcation in Arctic sea-ice cover we considered whether it was preceded (or followed) by any signals of destabilization in the form of critical slowing down. We note that the bifurcation inferred (Figs. 3, A2) represents the creation of a new ice cover state (in the fluctuations) rather than the total loss of stability of the existing ice 10 cover state. Hence the existing ice cover state may not show any destabilization prior to the bifurcation. Sure enough, prior to 2007 there is no consistent early warning signal of destabilization (Fig. 4c, e, g). The indicators all increased around the anomalous sea-ice maximum in 1996, but then they all declined toward 2007, consistent with our potential reconstruction (Fig. 3c). The only early warning signal prior to 2007 is a rise 15 in the DFA-indicator in analysis of sea ice extent (Fig. A3). Sensitivity analysis confirms this is the only robust increase across the three indicators and the two datasets, prior to 2007 (Fig. 5). Thus, there was no consistent early warning signal of critical slowing down before the bifurcation. Indeed the normal sea-ice state showed signs of increasing stability in the preceding decade.

20 The sea-ice retreat in 2007 caused abrupt increases in all the indicators, which have continued to rise since then (Fig. 4c, e, g). Sensitivity analysis reveals a robust upward trend in the DFA-indicator across the whole dataset (Fig. 4d), but no robust overall trend in the ACF-indicator or variance (Fig. 4b, f). These results are reproduced in analysis of sea-ice extent data (Fig. A3). The rise in the DFA-indicator is consistent 25 with the sea-ice having increasing “memory” of its earlier states due to critical slowing down (Livina and Lenton, 2007), and the somewhat different behavior of the ACF and DFA indicators could be explained by the different time scales used for their calculation. The ACF-indicator, based only on lag-1 autocorrelation (here from one day to the next),

TCD

6, 2621–2651, 2012

## A recent bifurcation in Arctic sea-ice cover

V. N. Livina and  
T. M. Lenton

[Title Page](#)

[Abstract](#)

[Introduction](#)

[Conclusions](#)

[References](#)

[Tables](#)

[Figures](#)

◀

▶

◀

▶

[Back](#)

[Close](#)

[Full Screen / Esc](#)

[Printer-friendly Version](#)

[Interactive Discussion](#)



## A recent bifurcation in Arctic sea-ice cover

V. N. Livina and  
T. M. Lenton

[Title Page](#)

[Abstract](#)

[Introduction](#)

[Conclusions](#)

[References](#)

[Tables](#)

[Figures](#)

[◀](#)

[▶](#)

[◀](#)

[▶](#)

[Back](#)

[Close](#)

[Full Screen / Esc](#)

[Printer-friendly Version](#)

[Interactive Discussion](#)



may be monitoring the behavior of fast decay modes unrelated to critical slowing down. The DFA-indicator in contrast is calculated on time scales up to 100 days, which should be long enough to capture the slowest recovery mode of the sea-ice.

We conclude that overall the indicators detect destabilization in 2007, which is ongoing, but do not forewarn of it.

Analysis of a much longer reconstruction of Arctic sea-ice extent since 1870 at annual resolution (Kinnard et al., 2011), shows a strong and robust upward trend in inter-annual variability (variance) of the sea-ice prior to recent retreats (Fig. 6), but no other early warning signals. Such increased variability of the sea-ice cover as it thins (Notz et al., 2009) could have encouraged recent transitions between ice cover states. This might support an alternative hypothesis that the low ice cover attractor already existed but only began to be sampled in 2007 and since, thanks to increasing internal variability.

### 3.3 Seasonal analysis

Our results may be sensitive to the fact that land masses mute variations in winter-spring ice area (Eisenman, 2010), whereas summer-autumn area is less affected. To address this we analyzed a derived index of “equivalent sea-ice extent” (Eisenman, 2010), which is based on the latitude of the sea-ice edge where it is free to migrate, converted to an area, assuming there were no continents present. Fluctuations are much larger in this index, and recent summer-autumn ice retreats no longer stand out as anomalous (Eisenman, 2010), hence no recent bifurcation is detected (Fig. A4). However, there is still a signal of overall destabilization (Fig. A5), which appears before the signal in actual sea-ice area (Fig. 4). This suggests our detection of a recent bifurcation in sea-ice cover could be (at least partly) a geographic property of the shrinkage of summer-autumn ice cover away from the continents facilitating larger fluctuations (Eisenman, 2010).

To examine whether this is the case, we looked at whether the new low ice cover state is just associated with summer-autumn intervals, by subdividing the original data

## A recent bifurcation in Arctic sea-ice cover

V. N. Livina and  
T. M. Lenton

Discussion Paper | Discussion Paper

Discussion Paper | Discussion Paper

Discussion Paper | Discussion Paper

[Title Page](#)

[Abstract](#)

[Introduction](#)

[Conclusions](#)

[References](#)

[Tables](#)

[Figures](#)

◀

▶

◀

▶

[Back](#)

[Close](#)

[Full Screen / Esc](#)

[Printer-friendly Version](#)

[Interactive Discussion](#)



(Fig. 1a) into two composite series; summer-autumn (June–November inclusive) and winter-spring (December–May inclusive), removing the mean cycle from each, and re-running the analysis. Both subsets of the data carry part of the signal of the inferred bifurcation in 2007 (Fig. 7), suggesting the sampling of an alternative attractor is not

5 a purely summer-autumn phenomenon. The signal is clearest in summer-autumn, but does not span as wide a range of window lengths as in the full data analysis. The summer-autumn (Fig. 8) and winter-spring (Fig. 9) data subsets also both show an overall rise in variance. However, only the summer-autumn data shows upward trends 10 in the ACF and DFA indicators (Fig. 8). Thus, the recent signal of slowing down (i.e. destabilization) is associated primarily with summer-autumn sea-ice fluctuations.

## 4 Conclusions

We present a conceptual model to try and explain recent sea-ice behavior in (Fig. 10), in which there is large seasonal forcing combined with a directional climate change forcing and stochastic variability. We hypothesize that combined effects of climate change 15 and seasonal forcing pushed the system past a bifurcation point in the summer of 2007 and in every summer since, to a low ice cover state, but the strong seasonal reduction in forcing each winter caused the sea-ice to revert to its normal state.

The appearance of a new lower ice cover state is consistent with positive feedbacks between ice cover and other climate variables becoming stronger (because to separate 20 two different stable states of a system under the same boundary conditions requires strong positive feedback). Several positive feedbacks have been identified in recent data. Sea-ice retreat since 1979 has exposed a dark ocean surface, causing 85 % of the Arctic region to receive an increase in solar heat input at the surface, with an increase of 5 % per year in some regions (Perovich et al., 2007). This is warming the upper Arctic ocean and contributing to melting on the bottom of the sea-ice (Perovich 25 et al., 2008). Sea-ice retreat is also amplifying warming of the lower atmosphere in the Arctic (Screen and Simmonds, 2010), which is shifting precipitation from snow

to rainfall, and where rain lands on the remaining sea ice cover, it is encouraging melt (Screen and Simmonds, 2011). Finally, sea-ice loss is beginning to change atmospheric circulation patterns (Overland and Wang, 2010) (although how that feeds back to ice cover is unclear).

5 The bifurcation we detect clearly does not involve total seasonal sea-ice loss hence is sub-Arctic in scale. There is a precedent for this; past abrupt Arctic cooling and warming events have been linked to switches between alternative states for sea-ice cover in the Barents and Kara Seas region (Bengtsson et al., 2004; Semenov et al., 2009). Such sub-Arctic-scale switches can still have significant impacts, indeed recent 10 ice loss from the Barents and Kara Seas has been linked to cold winter extremes over Eurasia (Petoukhov and Semenov, 2010). The connection between surface temperature sea level pressure and winds in the Arctic region and their effect on the sea-ice cover is discussed in the recent paper by Comiso (2012).

15 The detected ongoing destabilization of the summer-autumn sea-ice cover suggests that a further bifurcation may be approaching. Either the new low ice cover state is a transient feature and the system may revert to the normal ice cover state. Or there could be a further abrupt decrease in summer-autumn ice cover.

20 *Acknowledgements.* The research was supported by the NERC project “Detecting and classifying bifurcations in the climate system” (NE/F005474/1) and by the AXA Research Fund through a postdoctoral fellowship for V.N.L. Research was carried out on the High Performance Computing Cluster at the University of East Anglia. We thank J. Imbers Quintana and A. Lopes for discussions and M. Scheffer for suggesting the conceptual model.

## References

- 25 Abbot, D. S., Silber, M., and Pierrehumbert, R. T., Bifurcations leading to summer Arctic sea ice loss, *J. Geophys. Res.*, 116, D19120, doi:10.1029/2011JD015653, 2011. 2623  
Amstrup, S. C., DeWeaver, E. T., Douglas, D., Marcot, B. G., Durner, G. M., Bitz, C. M., and Bailey, D. A.: Greenhouse gas mitigation can reduce sea-ice loss and increase polar bear persistence, *Nature*, 468, 955–958, 2010. 2623

## A recent bifurcation in Arctic sea-ice cover

V. N. Livina and  
T. M. Lenton

[Title Page](#)

[Abstract](#) [Introduction](#)

[Conclusions](#) [References](#)

[Tables](#) [Figures](#)



[Back](#) [Close](#)

[Full Screen / Esc](#)

[Printer-friendly Version](#)

[Interactive Discussion](#)



- Bengtsson, L., Semenov, V. A., and Johannessen, O. M.: The early twentieth-century warming in the Arctic – a possible mechanism, *J. Climate*, 17, 4045–4057, 2004. 2633
- Boe, J., Hall, A., and Qu, X.: September sea-ice cover in the Arctic Ocean projected to vanish by 2100, *Nature Geosci.*, 2, 341–343, 2009. 2622
- 5 Cavalieri, D., Parkinson, C., Gloerson, P., and Zwally, H.: Sea ice concentrations from Nimbus-7 SMMR and DMSP SSM/I passive microwave data, 1978–2007, available at: <http://nsidc.org/data/nsidc-0051.html> (last access: 17 July 2012), Natl. Snow and Ice Data Center, Boulder, CO, 1996. 2624
- Comiso, J.: Large decadal decline of the Arctic multiyear ice cover, *J. Climate*, 25, 1176–1193, 10 2012. 2633
- Ditlevsen, P. D. and Johnsen, S. J.: Tipping points: early warning and wishful thinking, *Geophys. Res. Lett.*, 37, L19703, doi:10.1029/2010GL044486, 2010. 2628
- Eisenman, I.: Geographic muting of changes in the Arctic sea ice cover, *Geophys. Res. Lett.*, 37, L16501, doi:10.1029/2010GL043741, 2010. 2623, 2624, 2625, 2631, 2647, 2650
- 15 Eisenman, I. and Wettlaufer, J. S.: Nonlinear threshold behavior during the loss of Arctic sea ice. *Proc. Natl. Acad. Sci. USA*, 106, 28–32, 2009. 2623
- Held, H. and Kleinen, T.: Detection of climate system bifurcations by degenerate fingerprinting, *Geophys. Res. Lett.*, 31, L23207, doi:10.1029/2004GL020972, 2004. 2623, 2627, 2628
- Kendall, M. G.: *Rank Correlation Methods*, Charles Griffin and Company Limited, London, 1948. 20 2628
- Kinnard, C., Zdanowicz, C. M., Fisher, D. A., Isaksson, E., de Vernal, A., and Thompson, L. G.: Reconstructed changes in Arctic sea ice over the past 1450 years, *Nature*, 479, 509–512, 2011. 2631, 2642
- Lenton, T. M.: Early warning of climate tipping points, *Nature Clim. Change*, 1, 201–209, 2011. 25 2623
- Lenton, T. M., Held, H., Kriegler, E., Hall, J. W., Lucht, W., Rahmstorf, S., and Schellnhuber, H. J.: Tipping elements in the Earth's climate system, *Proc. Nat. Acad. Sci. USA*, 105, 1786–1793, 2008. 2623
- Lindsay, R. W. and Zhang, J.: The thinning of Arctic sea ice, 1988–2003: have we passed a tipping point?, *J. Climate*, 18, 4879–4894, 2005. 2623
- 30 Livina, V. N. and Lenton, T. M.: A modified method for detecting incipient bifurcations in a dynamical system, *Geophys. Res. Lett.*, 34, L03712, doi:10.1029/2006GL028672, 2007. 2623, 2627, 2628, 2630

## A recent bifurcation in Arctic sea-ice cover

V. N. Livina and  
T. M. Lenton

[Title Page](#)

[Abstract](#)

[Introduction](#)

[Conclusions](#)

[References](#)

[Tables](#)

[Figures](#)

◀

▶

◀

▶

[Back](#)

[Close](#)

[Full Screen / Esc](#)

[Printer-friendly Version](#)

[Interactive Discussion](#)



## A recent bifurcation in Arctic sea-ice cover

V. N. Livina and  
T. M. Lenton

- Livina, V. N., Kwasniok, F., and Lenton, T. M.: Potential analysis reveals changing number of climate states during the last 60 kyr, *Clim. Past*, 6, 77–82, doi:10.5194/cp-6-77-2010, 2010. 2623, 2625, 2626
- 5 Livina, V. N., Ditlevsen, P. D., and Lenton, T. M.: An independent test of methods of detecting and anticipating bifurcations in time-series data, *Phys. A Stat. Mech. Appl.*, 391, 485–496, doi:10.1016/j.physa.2011.08.025, 2011a. 2625
- Livina, V. N., Kwasniok, F., Lohmann, G., Kantelhardt, J. W., and Lenton, T. M.: Changing climate states and stability: from Pliocene to present, *Clim. Dynam.*, 37, 2437–2453, 2011b. 2623, 2625, 2626, 2629, 2639
- 10 Maslanik, J. and Stroeve, J.: Near real-time DMSP SSM/I daily polar gridded sea ice concentrations, available at: <http://nsidc.org/data/nsidc-0081.html> (last access: 17 July 2012), Natl. Snow and Ice Data Center, Boulder, CO, 1999. 2624
- Meier, W., Fetterer, F., Knowles, K., Savoie, M., and Brodzik, M. J.: Sea ice concentrations from Nimbus-7 SMMR and DMSP SSM/I passive microwave data, January–December 2008, 15 available at: <http://nsidc.org/data/nsidc-0051.html>, Natl. Snow and Ice Data Center, Boulder, CO, 2006. 2624
- Nghiem, S. V., Rigor, I. G., Perovich, D. K., Clemente-Colon, P., Weatherly, J. W., and Neumann, G.: Rapid reduction of Arctic perennial sea ice, *Geophys. Res. Lett.*, 34, L19504, doi:10.1029/2007GL031138, 2007. 2622
- 20 Notz, D.: The future of ice sheets and sea ice: between reversible retreat and unstoppable loss, *Proc. Natl. Acad. Sci. USA*, 106, 20590–20595, 2009. 2623, 2631
- Overland, J. E. and Wang, M.: Large-scale atmospheric circulation changes are associated with the recent loss of Arctic sea ice, *Tellus A*, 62, 1–9, 2010. 2633
- 25 Perovich, D. K., Light, B., Eicken, H., Jones, K. F., Runciman, K., and Nghiem, S. V.: Increasing solar heating of the Arctic Ocean and adjacent seas, 1979–2005: Attribution and role in the ice-albedo feedback, *Geophys. Res. Lett.*, 34, L19505, doi:10.1029/2007GL031480, 2007. 2632
- Perovich, D. K., Richter-Menge, J. A., Jones, K. F., and Light, B.: Sunlight, water, and ice: extreme Arctic sea ice melt during the summer of 2007, *Geophys. Res. Lett.*, 35, L11501, 30 doi:10.1029/2008GL034007, 2008. 2632
- Petoukhov, V. and Semenov, V. A.: A link between reduced Barents-Kara sea ice and cold winter extremes over northern continents, *J. Geophys. Res.*, 115, D21111, doi:10.1029/2009JD013568, 2010. 2633

Discussion Paper | Discussion Paper

[Title Page](#)

[Abstract](#)

[Introduction](#)

[Conclusions](#)

[References](#)

[Tables](#)

[Figures](#)



[Back](#)

[Close](#)

[Full Screen / Esc](#)

[Printer-friendly Version](#)

[Interactive Discussion](#)



- Scheffer, M., Bascompte, J., Brock, W. A., Brovkin, V., Carpenter, S. R., Dakos, V., Held, H., van Nes, E. H., Rietkerk, M., and Sugihara, G.: Early warning signals for critical transitions, *Nature*, 461, 53–59, 2009. 2623, 2627
- Screen, J. A. and Simmonds, I.: The central role of diminishing sea ice in recent Arctic temperature amplification, *Nature*, 464, 1334–1337, 2010. 2632
- Screen, J. and Simmonds, I.: Declining summer snowfall in the Arctic: causes, impacts and feedbacks, *Clim. Dynam.*, 38, 2243–2256, doi:doi:10.1007/s00382-011-1105-2, 2011. 2633
- Semenov, V. A., Park, W., and Latif, M.: Barents Sea inflow shutdown: a new mechanism for rapid climate changes, *Geophys. Res. Lett.*, 36, L14709, doi:10.1029/2009GL038911, 2009. 2633
- Stroeve, J., Holland, M. M., Meier, W., Scambos, T., and Serreze, M.: Arctic sea ice decline: faster than forecast, *Geophys. Res. Lett.*, 34, L09501, doi:10.1029/2007GL029703, 2007. 2622
- Tietsche, S., Notz, D., Jungclaus, J. H., and Marotzke, J.: Recovery mechanisms of Arctic summer sea ice, *Geophys. Res. Lett.*, 38, L02707, doi:10.1029/2010GL045698, 2011. 2623
- Winton, M.: Does the Arctic sea ice have a tipping point?, *Geophys. Res. Lett.*, 33, L23504, doi:10.1029/2006GL028017, 2006. 2623

Discussion Paper | Discussion Paper

Discussion Paper | Discussion Paper

Discussion Paper | Discussion Paper

## A recent bifurcation in Arctic sea-ice cover

V. N. Livina and  
T. M. Lenton

[Title Page](#)[Abstract](#)[Introduction](#)[Conclusions](#)[References](#)[Tables](#)[Figures](#)[◀](#)[▶](#)[◀](#)[▶](#)[Back](#)[Close](#)[Full Screen / Esc](#)[Printer-friendly Version](#)[Interactive Discussion](#)

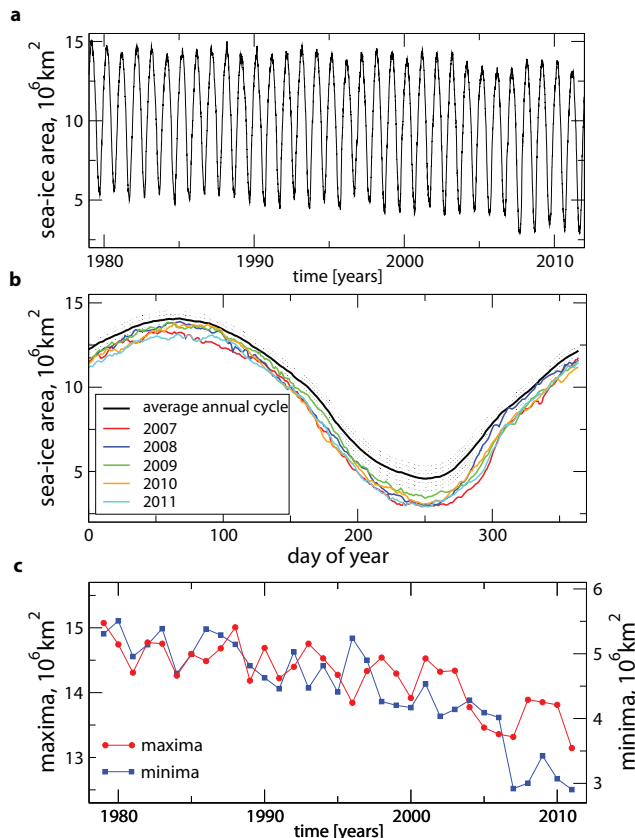


**Fig. 1.** Arctic sea-ice area from satellite data. **(a)** Arctic sea-ice area, 1979–2012. **(b)** The mean annual cycle of the area data over 1979–2008 inclusive (solid line, shaded area denotes two error bars), together with the last five anomalous years. **(c)** Annual maxima (left axis) and minima (right axis) showing an abrupt increase in amplitude of the seasonal cycle in 2007.

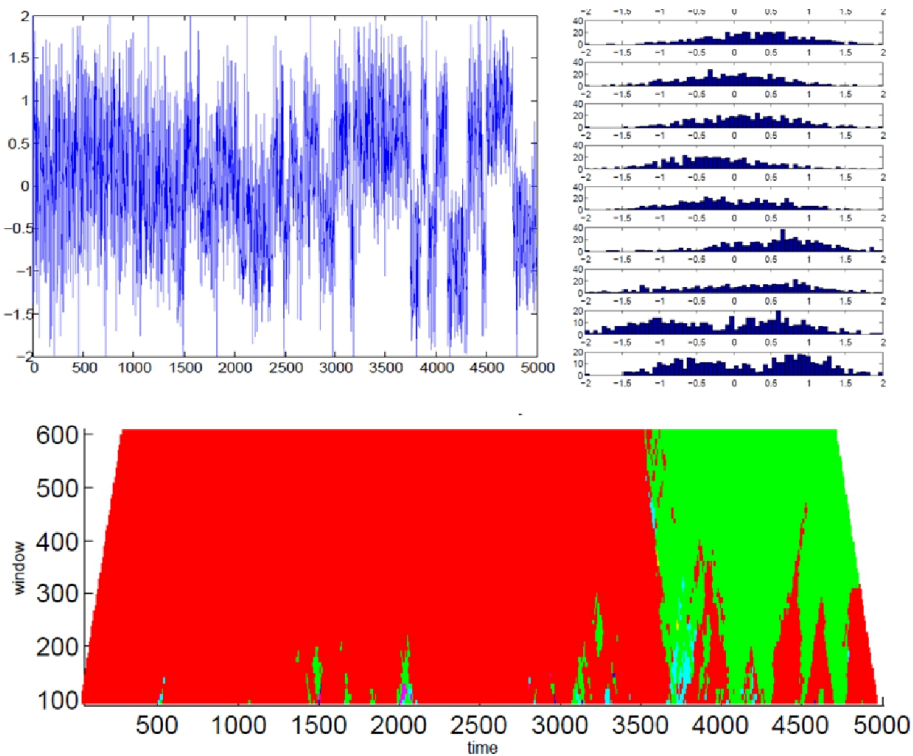


**Fig. 2.** Test of potential analysis on artificial data from a system bifurcating from one state to two. Here the underlying potential changes smoothly from one-well to double-well, described by the stochastic potential equation with varying potential wells (10 chunks of 500 points each), with the bifurcation occurring at time 3500. **(a)** artificial data generated from the changing potential function with a noise level 1; **(b)** histograms of 10 chunks of data, from top to bottom, corresponding to consequent subsets of the series **(c)** Contour plot of number of detected states, where red = 1 detected state, green = 2. Results plotted as a function of sliding window length at the middle of the window.

## A recent bifurcation in Arctic sea-ice cover

V. N. Livina and  
T. M. Lenton

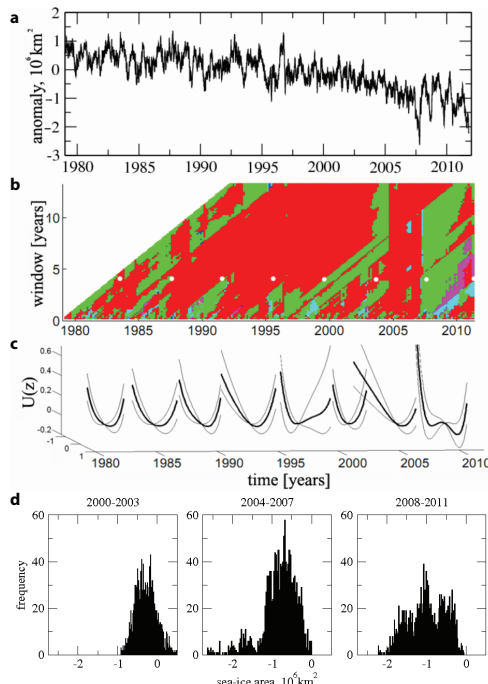


**Fig. 3.** Detection of a bifurcation in Arctic sea-ice area. **(a)** Sea-ice area anomaly, daily data with mean seasonal cycle removed. **(b)** Contour plot of number of detected states, where red = 1 detected state, green = 2, cyan = 3, magenta = 4. Results plotted as a function of sliding window length at the end of the window. **(c)** Reconstructed potential curves of eight 4-yr time intervals, corresponding to the white dots in **(b)**. Here “z” is sea-ice area fluctuation on a shifted scale. Faint lines are potential curves derived from error estimates on the coefficients of the polynomial potential function (for details see Livina et al., 2011b). In the penultimate interval 2004–2007 a second state starts to appear and in the final interval 2008–2011 there are two states of comparable stability. **(d)** Histograms of the data for 2000–2003, 2004–2007, 2008–2011 from which the corresponding potential curves are derived (see Methods).

[Title Page](#)

[Abstract](#)

[Introduction](#)

[Conclusions](#)

[References](#)

[Tables](#)

[Figures](#)

[◀](#)

[▶](#)

[◀](#)

[▶](#)

[Back](#)

[Close](#)

[Full Screen / Esc](#)

[Printer-friendly Version](#)

[Interactive Discussion](#)

## A recent bifurcation in Arctic sea-ice cover

V. N. Livina and  
T. M. Lenton

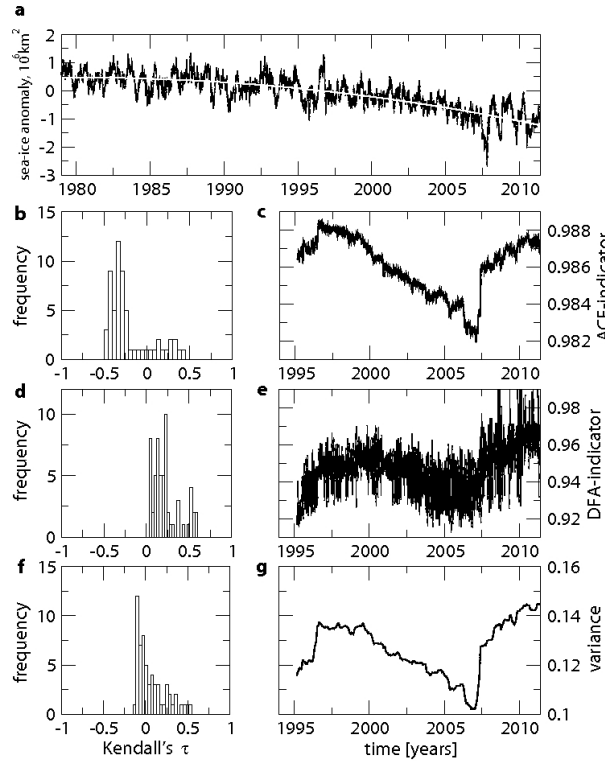


**Fig. 4.** Search for early warning signals of bifurcation in Arctic sea-ice area data. **(a)** Sea-ice area anomaly (as in Fig. 2a) showing the quadratic downward trend that is removed prior to calculating the instability indicators. Right panels show example indicators using a sliding window of length half the series, with results plotted at the end of the sliding window. Indicators from: **(c)** autocorrelation function (ACF), **(e)** detrended fluctuation analysis (DFA) and **(g)** variance. Left panels show histograms of the Kendall statistic for the trend in the indicators when varying the sliding window length from 1/4 to 3/4 of the series: **(b)** ACF-indicator, **(d)** DFA-indicator, **(f)** variance.

[Title Page](#)

[Abstract](#)

[Introduction](#)

[Conclusions](#)

[References](#)

[Tables](#)

[Figures](#)

◀

▶

◀

▶

[Back](#)

[Close](#)

[Full Screen / Esc](#)

[Printer-friendly Version](#)

[Interactive Discussion](#)

## A recent bifurcation in Arctic sea-ice cover

V. N. Livina and  
T. M. Lenton

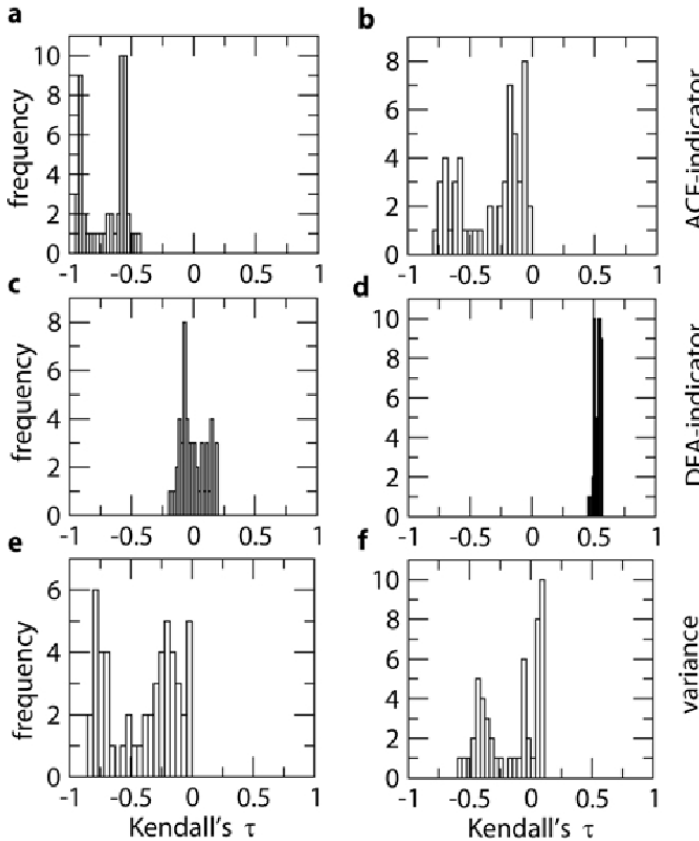


**Fig. 5.** Destabilisation indicators calculated up to 2007. From; **(a, c, e)** sea-ice area anomaly, **(b, d, f)** sea-ice extent anomaly (both after detrending). Sensitivity analysis when varying sliding window length for Kendall trend statistic of: **(a, b)** ACF-indicator **(c, d)** DFA-indicator **(e, f)** variance.

## A recent bifurcation in Arctic sea-ice cover

V. N. Livina and  
T. M. Lenton

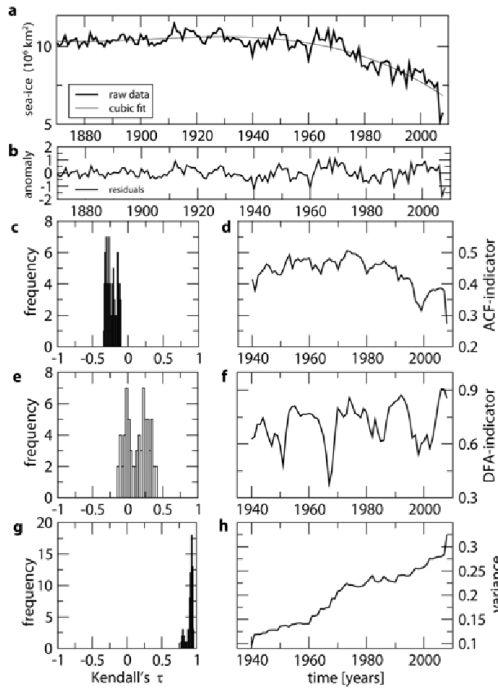


**Fig. 6.** Destabilisation indicators calculated in annual reconstructed sea-ice extent from 1870. **(a)** Reconstructed sea-ice extent (from Kinnard et al., 2011) showing the cubic trend that is removed prior to calculating the instability indicators. **(b)** The residuals after removing the trend, which are analysed. Right panels show example indicators from: **(d)** autocorrelation function (ACF), **(f)** detrended fluctuation analysis (DFA) and **(h)** variance, results plotted at end of a sliding window of length half the series. Left panels show histograms of the Kendall  $\tau$  statistic for the trend in the indicators when varying the sliding window length from 1/4 to 3/4 of the series: **(c)** ACF-indicator, **(e)** DFA-indicator, **(g)** variance. Note that the record has too few data points to get reliable results for the DFA-indicator.

## A recent bifurcation in Arctic sea-ice cover

V. N. Livina and  
T. M. Lenton

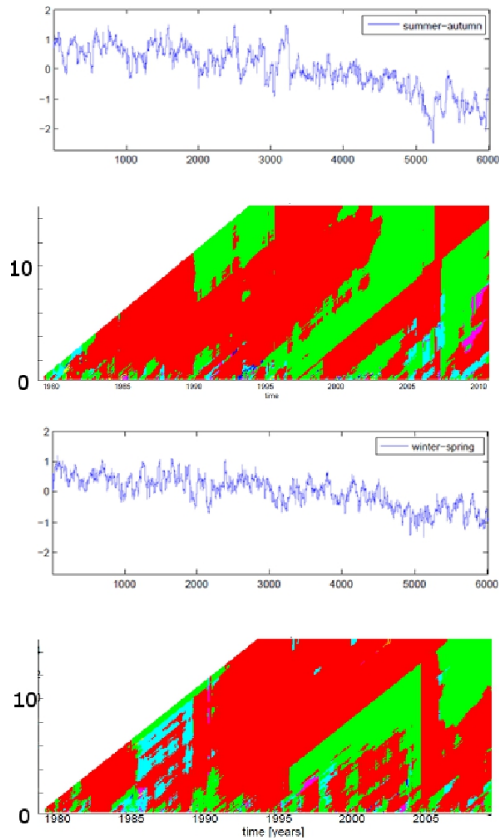


**Fig. 7.** Potential analysis of summer-autumn and winter-spring Arctic sea-ice area data. **(a)** Summer-autumn sea-ice area anomaly, daily data with mean cycle removed. **(b)** Contour plot of number of detected states. **(c)** Winter-spring sea-ice area anomaly, daily data with mean cycle removed. **(d)** Contour plot of number of detected states.

## A recent bifurcation in Arctic sea-ice cover

V. N. Livina and  
T. M. Lenton

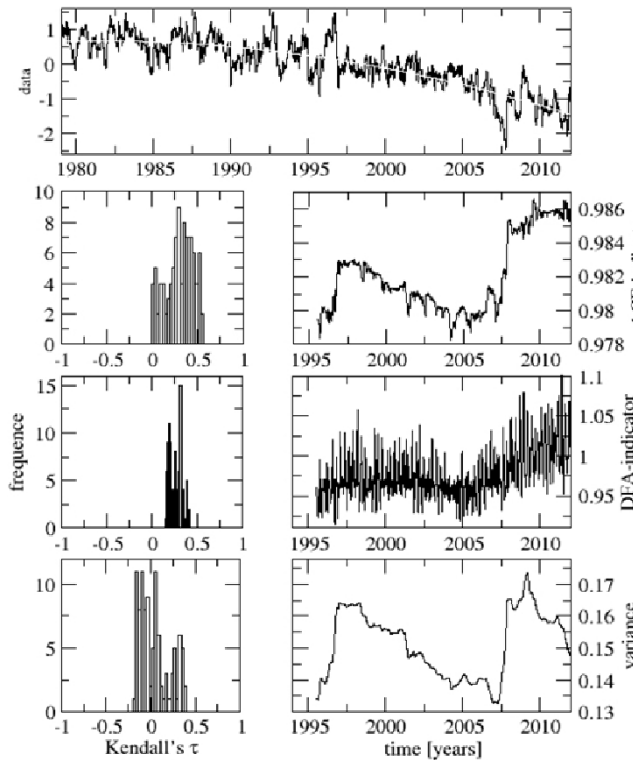


**Fig. 8.** Search for early warning signals of bifurcation in summer-autumn Arctic sea-ice area. **(a)** Summer-autumn sea-ice area anomaly (as in Fig. A3a) showing the quadratic downward trend that is removed prior to calculating the instability indicators. Right panels show example indicators from: **(c)** autocorrelation function (ACF), **(e)** detrended fluctuation analysis (DFA) and **(g)** variance, results plotted at end of a sliding window of length half the series. Left panels show histograms of the Kendall statistic for the trend in the indicators when varying the sliding window length from 1/4 to 3/4 of the series: **(b)** ACF-indicator, **(d)** DFA-indicator, **(f)** variance.

[Title Page](#)[Abstract](#)[Introduction](#)[Conclusions](#)[References](#)[Tables](#)[Figures](#)[Back](#)[Close](#)[Full Screen / Esc](#)[Printer-friendly Version](#)[Interactive Discussion](#)

## A recent bifurcation in Arctic sea-ice cover

V. N. Livina and  
T. M. Lenton

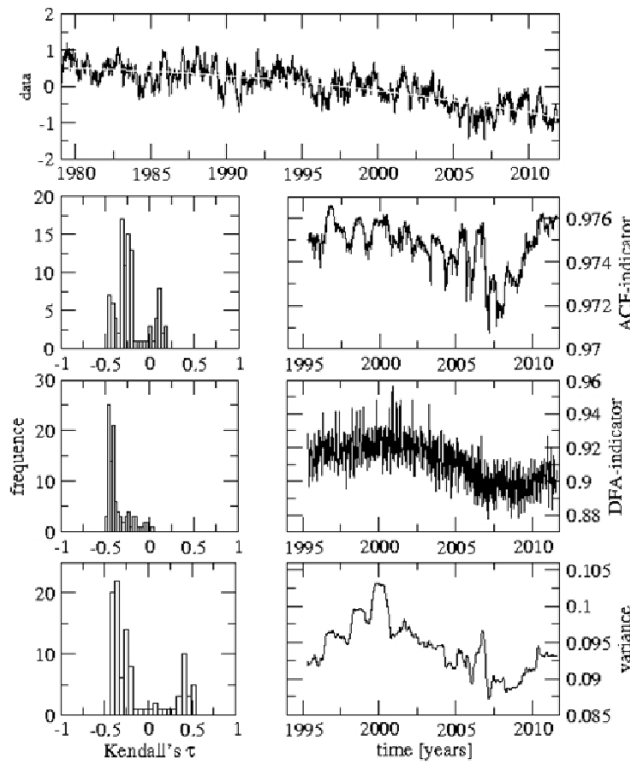


**Fig. 9.** Search for early warning signals of bifurcation in winter-spring Arctic sea-ice area. **(a)** Winter-spring sea-ice area anomaly (as in Fig. A3c) showing the quadratic downward trend that is removed prior to calculating the instability indicators. Right panels show example indicators from: **(c)** autocorrelation function (ACF), **(e)** detrended fluctuation analysis (DFA) and **(g)** variance, results plotted at end of a sliding window of length half the series. Left panels show histograms of the Kendall statistic for the trend in the indicators when varying the sliding window length from 1/4 to 3/4 of the series: **(b)** ACF-indicator, **(d)** DFA-indicator, **(f)** variance.

## A recent bifurcation in Arctic sea-ice cover

V. N. Livina and  
T. M. Lenton

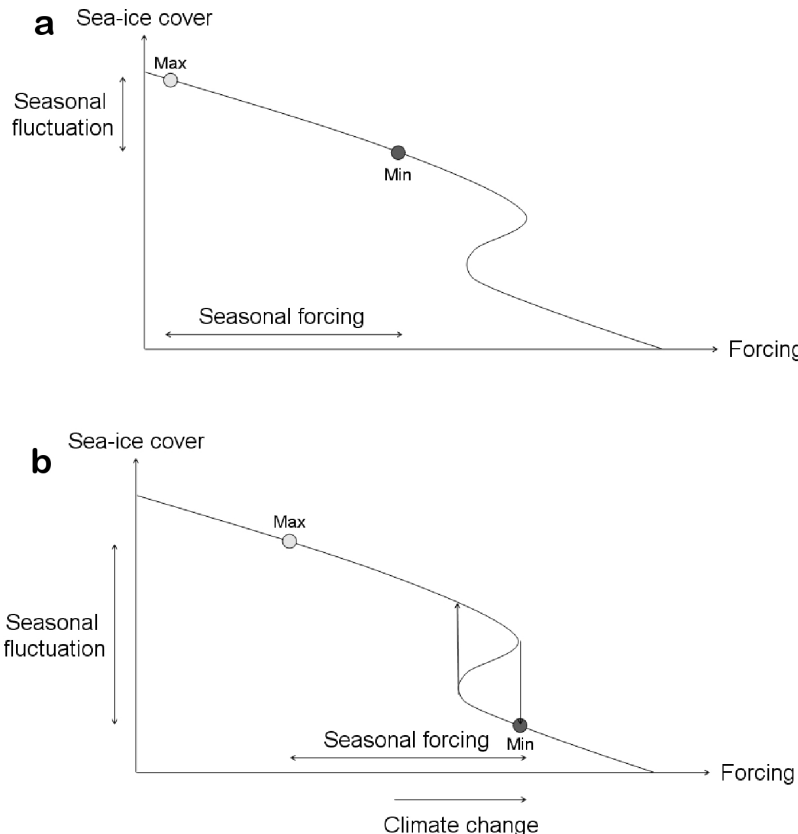


**Fig. 10.** Schematic model of sea-ice dynamics with changes exaggerated: **(a)** before bifurcation, showing range of seasonal forcing and seasonal response of normal ice cover state, and **(b)** after climate change forcing, the system passes a bifurcation in summer to an alternative lower ice cover state, but reverts later in the season to the normal ice cover state.

[Title Page](#)

[Abstract](#)

[Introduction](#)

[Conclusions](#)

[References](#)

[Tables](#)

[Figures](#)

[◀](#)

[▶](#)

[◀](#)

[▶](#)

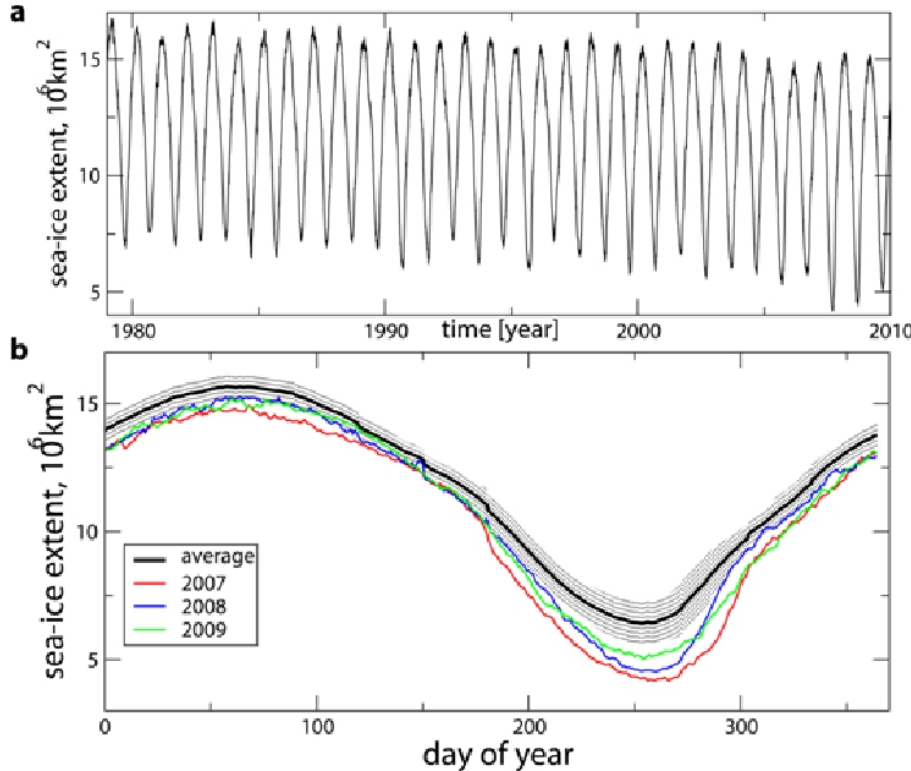
[Back](#)

[Close](#)

[Full Screen / Esc](#)

[Printer-friendly Version](#)

[Interactive Discussion](#)

**A recent bifurcation  
in Arctic sea-ice  
cover**V. N. Livina and  
T. M. Lenton

**Fig. A1.** Arctic sea-ice extent from satellite data. **(a)** Arctic sea-ice extent from Eisenman (Eisenman, 2010) <ftp://ftp.agu.org/apend/gl/2010gl043741>. **(b)** The mean annual cycle of the extent data over 1979–2009 (solid line, shaded area denotes  $2\sigma$  error bars), together with the last three anomalous years.

Title Page

Abstract

Introduction

Conclusions

References

Tables

Figures



Back

Close

Full Screen / Esc

Printer-friendly Version

Interactive Discussion

## A recent bifurcation in Arctic sea-ice cover

V. N. Livina and  
T. M. Lenton

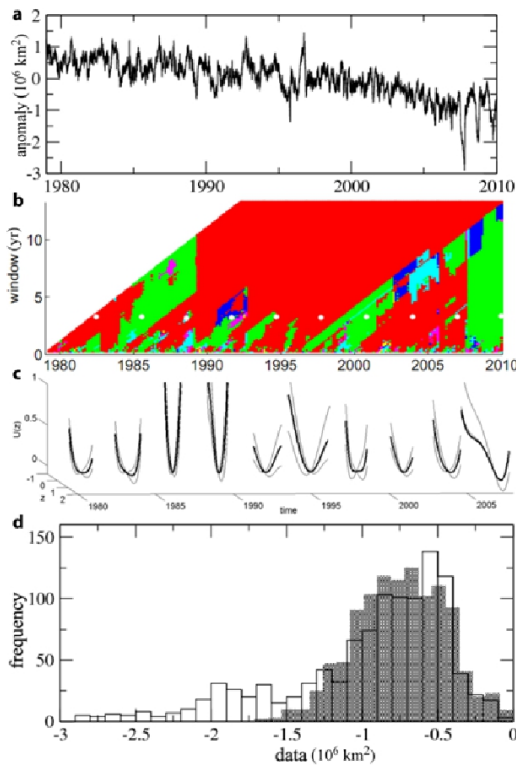


**Fig. A2.** Detection of a recent bifurcation in Arctic sea-ice extent. **(a)** Sea-ice extent anomaly, daily data with mean seasonal cycle removed. **(b)** Contour plot of number of detected states, where red = 1 detected state, green = 2, cyan = 3, magenta = 4. Results plotted as a function of sliding window length at the end of the window. **(c)** Reconstructed potential curves of ten 3-yr time intervals, corresponding to the white dots in **(b)**. In the final interval 2007–2009 a second (degenerate) state appears. **(d)** Histograms of the data for 2004–2006 (shaded) and 2007–2009 (unshaded), from which the corresponding potential curves are derived, showing the appearance of a second mode among a long-tail of negative anomalies.

## A recent bifurcation in Arctic sea-ice cover

V. N. Livina and  
T. M. Lenton

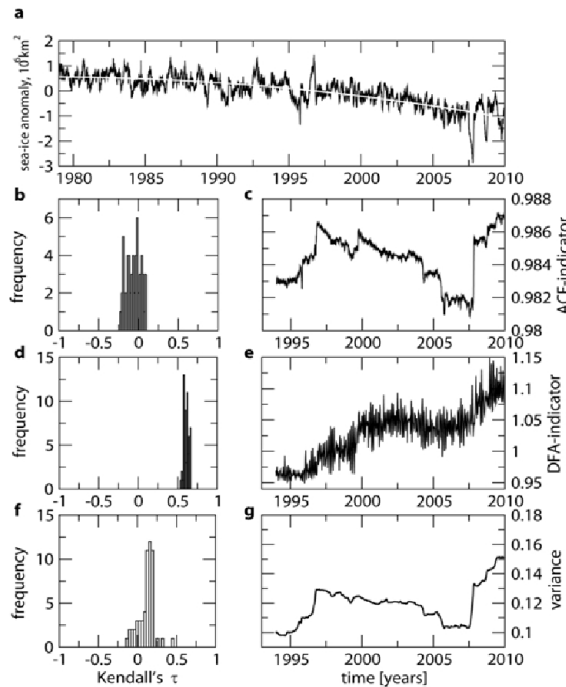


**Fig. A3.** Search for early warning signals of bifurcation in Arctic sea-ice extent data. **(a)** Sea-ice extent anomaly (as in Fig. 2a) showing the quadratic downward trend that is removed prior to calculating the instability indicators. Right panels show example indicators from: **(c)** autocorrelation function (ACF), **(e)** detrended fluctuation analysis (DFA) and **(g)** variance, results plotted at end of a sliding window of length half the series. Left panels show histograms of the Kendall statistic for the trend in the indicators when varying the sliding window length from 1/4 to 3/4 of the series: **(b)** ACF-indicator, **(d)** DFA-indicator, **(f)** variance.

[Title Page](#)

[Abstract](#) [Introduction](#)

[Conclusions](#) [References](#)

[Tables](#) [Figures](#)



[Full Screen / Esc](#)

[Printer-friendly Version](#)

[Interactive Discussion](#)

## A recent bifurcation in Arctic sea-ice cover

V. N. Livina and  
T. M. Lenton

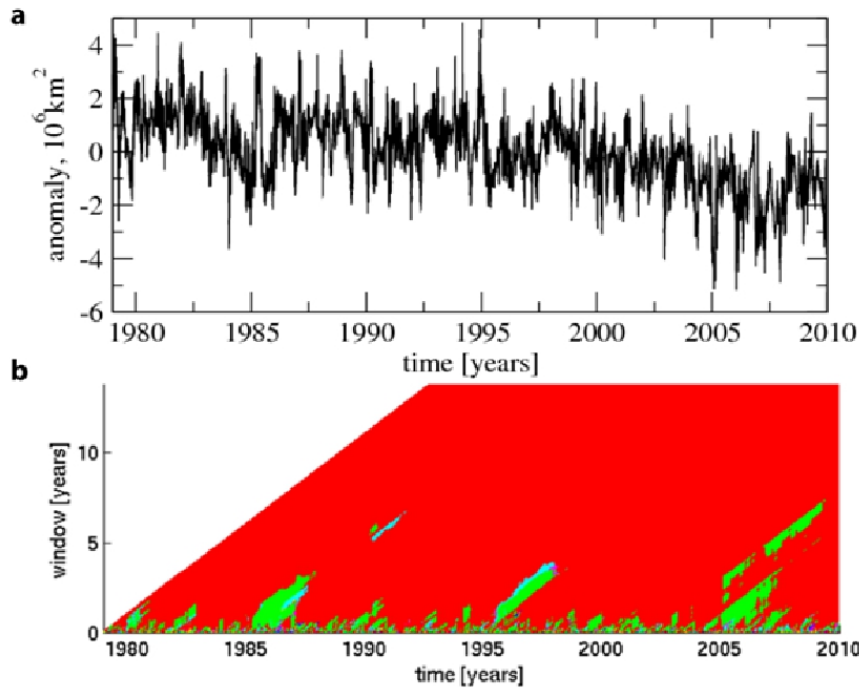


**Fig. A4.** Potential analysis of equivalent sea-ice extent index. **(a)** Dataset constructed by Eisenman (Eisenman, 2010) and available at: <ftp://ftp.agu.org/apend/gl/2010gl043741>, which is based on the latitude of the Arctic sea ice edge where the ice is free to migrate, converted to an equivalent area, assuming there were no land masses in the high northern latitudes. **(b)** Contour plot of number of detected states, where red = 1 detected state, green = 2, cyan = 3, magenta = 4. Results plotted as a function of sliding window length at the end of the window. No bifurcation is detected in this dataset, because it has much higher internal variability (Fig. 6g) than sea ice extent (Fig. A3g) and recent observed ice extent anomalies are dwarfed by earlier, larger fluctuations that are inferred would have occurred had the continents not got in the way of winter ice variations.

[Title Page](#) | [Abstract](#) | [Introduction](#)  
[Conclusions](#) | [References](#)  
[Tables](#) | [Figures](#)  
[◀](#) | [▶](#)  
[◀](#) | [▶](#)  
[Back](#) | [Close](#)  
[Full Screen / Esc](#)  
[Printer-friendly Version](#)  
[Interactive Discussion](#)

## A recent bifurcation in Arctic sea-ice cover

V. N. Livina and  
T. M. Lenton

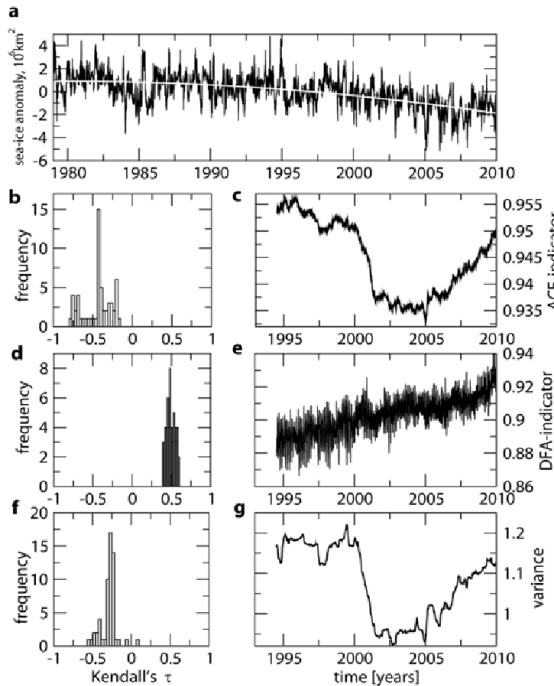


**Fig. A5.** Search for signals of destabilisation in equivalent sea-ice extent. **(a)** Equivalent sea-ice extent index (as in Fig. A2) showing the quadratic downward trend that is removed prior to calculating the instability indicators. Right panels show example indicators from: **(c)** autocorrelation function (ACF), **(e)** detrended fluctuation analysis (DFA) and **(g)** variance; results plotted at end of a sliding window of length half the series. Left panels show histograms of the Kendall  $\tau$  statistic for the trend in the indicators when varying the sliding window length from 1/4 to 3/4 of the series: **(b)** ACF-indicator, **(d)** DFA-indicator, **(f)** variance.

[Title Page](#)

[Abstract](#)

[Introduction](#)

[Conclusions](#)

[References](#)

[Tables](#)

[Figures](#)

[◀](#)

[▶](#)

[◀](#)

[▶](#)

[Back](#)

[Close](#)

[Full Screen / Esc](#)

[Printer-friendly Version](#)

[Interactive Discussion](#)